

THERMAL BENDING OF COPPER COOLING STAVES IN BLAST FURNACES*

Cameron Soltys ¹
Maher Al-Dojayli ²
Hamid Ghorbani ³

Abstract

Cooling staves in blast furnaces are used to minimize the process heat loads on steel shell and refractory system. Copper staves are exposed to significant fluctuating thermal loads which may lead to premature stave failures due to cracks, water leakage, bending, abrasion and resultant wear. In this paper, an assessment methodology is presented to evaluate the effect of thermal cycling on copper staves including bending, fatigue and thermal ratcheting. This approach incorporates temperature-dependent copper properties including creep and plasticity to more accurately capture inelastic deformations, damage and fatigue in staves under transient and cyclic thermal loading conditions. Root cause failure assessment and improvements to copper stave design can be assessed using the presented methodology.

Keywords: Blast Furnace; Copper Staves; Stave Damage; Thermal Bending.

¹ BAsC University of Waterloo, Mechanical EIT, Specialized Engineering Analysis and Design, Hatch, Mississauga, Ontario, Canada.

² Ph.D., MSc, BSc, University of Toronto, Specialist, Specialized Engineering Analysis and Design, Hatch, Mississauga, Ontario, Canada.

³ Ph.D., MAsC, BAsC, University of Toronto, Global Director, Specialized Engineering Analysis and Design, Hatch, Mississauga, Ontario, Canada.

1 INTRODUCTION

Copper staves installed in a blast furnace are exposed to a demanding thermal and mechanical environment. Cooling systems using staves are required to protect the furnace's steel shell from high process temperatures, and in doing so, prolong the campaign life of the furnace. Copper staves are typically installed in high-heat load areas of the furnace such as the bosh and lower stack. They are superior to the traditional cast iron staves due to their increased cooling intensity which can, in principle, result in a thicker protective accretion layer. In addition, copper staves can be thinner than cast iron, increasing the working volume of the blast furnace.

Copper staves were introduced to extend the campaign life of blast furnaces to 20 years. Some blast furnaces reported premature wear and failure of copper staves while others had long service life [1] [2]. In 2013, the worldsteel Technology Committee initiated a project to analyze 36 blast furnaces with the aim to understand performance issues related to copper stave life. Of the 36 furnaces, with varying size and shape, 13 experienced excessive wear and short stave life [2]. Most of these failures were caused by wear and cracking of the staves when exposed to normal blast furnace operating conditions. Some staves were excessively deformed, suggesting deformation/bending to be an additional contributing factor to the observed failures.

The worldsteel Technology Committee found that several blast furnace design factors - such as bosh angle, bosh height, and the shape and location of the stave - were correlated to stave wear. Although stave bending was mentioned as a factor affecting wear, it was mainly linked to mounting bolt and water-cooling pipe cracking [2].

A detailed thermomechanical assessment of a blast furnace copper stave is described using finite element analysis (FEA). A deep understanding of the behavior of a copper stave under conditions experienced in a blast furnace is developed to accurately estimate the deformation of the copper stave and the loads applied to the fixing pins. Our analysis considered transient thermal loads, temperature-dependent material properties, and non-linear copper properties such as creep and plasticity. The results can be applied to root cause failure assessments and to improve copper stave design through a better understanding of the causes of common failure mechanisms.

2 DEVELOPMENT

2.1 Background

Modern blast furnaces achieve production rates greater than 3.0 tonnes of hot metal per cubic meter of working volume per day [3]. This is accomplished using improved burden materials, burden distribution techniques, process control, high hot blast temperatures, oxygen enrichment, and pulverized coal and/or natural gas injection. Such a high blast furnace productivity can lead to elevated heat loads and heat load fluctuations at the furnace walls.

Blast furnace designs and operational conditions vary significantly between furnaces and over the life of a furnace, creating different conditions that copper staves experience. These include geometric design, thermal loading, mechanical loading, and deformation. Efforts can be found in the literature to investigate stave deformation through thermomechanical models and to determine stave behavior, accounting for various combinations of the following factors: stave geometry, a variety of heat load conditions,

mechanical loads from the burden, and stave plasticity and creep [2] [3] [4] [5]. By not considering all the factors at once, one may underestimate the amount of bending and the resulting damage. The approach presented in this paper will expand on these efforts by assessing the stave deformation accounting for all these variables. The model evaluates multiple transient scenarios to represent various furnace operating conditions.

The approach presented is based on steady-state and transient thermal analysis and temperature-dependent structural analysis using FEA techniques. These findings help guide the design of copper staves and/or mitigate some of the reported common failures in copper staves, namely fixing bolt cracking, banana effect, and stave hot face cracking.

2.1.1 Stave Deformation and the Banana Effect

Copper staves can deform due to the heat loads and thermal fluctuations experienced at the furnace walls due to changing blast furnace process conditions. These deformations are primarily due to the thermal expansion of the stave while being mechanically constrained by pins, fixing bolts, pipe connections, and grout.

A temperature gradient forms across the stave body when the working surface - facing the inside of the furnace - is subjected to an elevated heat load while the inner surface remains cool; this causes non-uniform thermal expansion and outward bending. If there is a gap or no grout between the stave and furnace shell, the stave is free to move/bend due to thermal expansion effects, as shown in Figure 1.

When the heat load is reduced, stave bending decreases and the stave returns close to its original shape. The ability of the stave to return to its original shape depends on the extent of the generated plastic strain.

An alternative deformation pattern observed in copper staves is the “banana effect” in which staves deform inward, toward the center of the furnace. This deformation occurs when the stave bending is restricted by the presence of stiff grout that restricts stave movement during the high heat load cycles, as shown in Figure 1. In this case, high thermal stresses are developed beyond the yield stress of the copper, creating plastic and creep strain zones. Once the operating conditions return the stave to a lower temperature, the thermal stresses in the stave relax by deforming/bending the stave into the furnace to reach a state of internal force equilibrium.

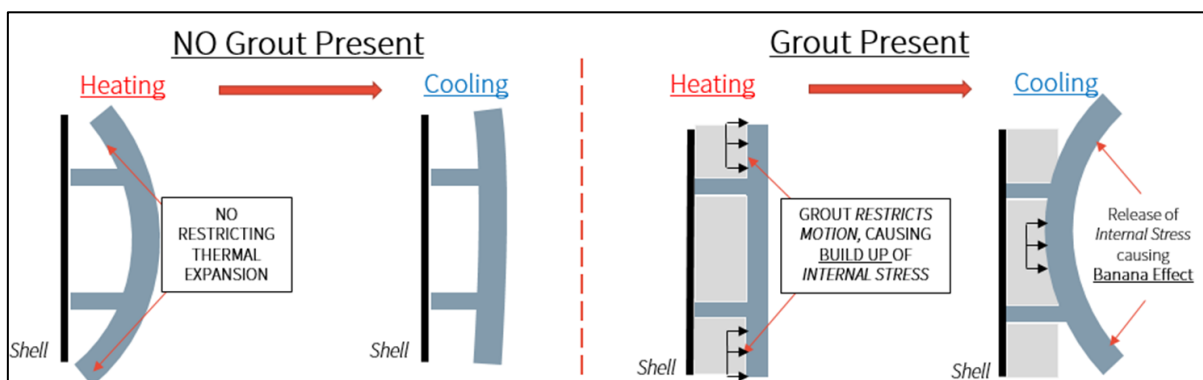


Figure 1. Expected deformation profile of a stave due to thermal stress

As seen in Figure 2, both deformation mechanisms can be described by the stave model that has been developed, depending on the details of the furnace design and operation. This analysis shows that the initial bending deformation of the stave depends on the presence of the grout and that this is a critical factor to consider when designing a stave

cooling system. In this paper, the “banana effect” deformation experienced by some copper staves will be investigated in detail. The developed stove model can produce other types of deformation, as seen in Figure 2, depending on the conditions of the furnace.

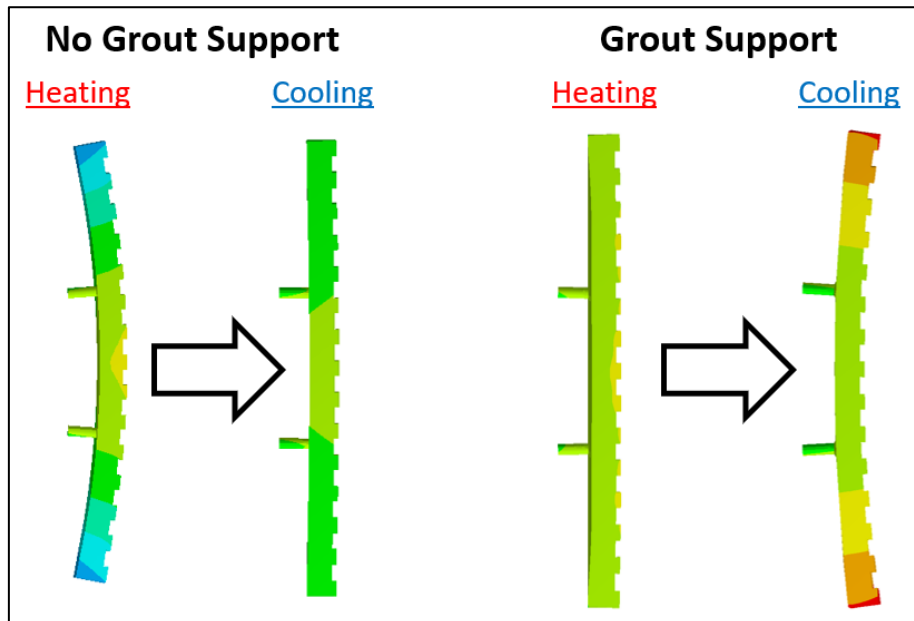


Figure 2. Expected deformation profiles replicated by the stove model (deformation exaggerated x10)

2.2 Methodology

Finite element thermomechanical models were developed to calculate the temperature, deformation, creep strain, and stress in generic copper stove designs subjected to cyclic heating scenarios. Two different stove geometries were considered to represent and compare typical stove sizes. Representative heating scenarios were applied to the staves, which were established based on copper stove thermocouple and cooling water temperature/flow data in the furnace bosh and belly regions.

Steady-state thermal analysis was used to verify the observed heat loads. Multiple transient thermal scenarios were analyzed to represent blast furnace operating conditions. The frequency of thermocouple measurements was used to determine if the response time would accurately capture abrupt and high heat load conditions.

The temperature-dependent thermal properties of a copper stove were used to accurately capture the effect of the variable transient heat loading scenarios. Temperature results of the copper stove body were mapped to the structural FEA model to conduct a thermomechanical analysis and estimate the behavior of the stove under these conditions. The structural model included the temperature- and time-dependent material properties of copper including elasticity, plasticity, and creep. Sensitivity analyses were conducted to evaluate the effect of the model mesh sizing and the variation in material properties on the deformation results.

Two different stove geometries were analyzed and compared, as seen in Figure 3. Stave B is twice the length of Stave A; both are representative of staves used in the industry. The fixing bolts are also in distinct locations since the bolts on stave B are further apart from each other. Initial analysis suggests that the critical dimension for bolt location is the distance from the end of the stove; the two staves are identical in this respect.

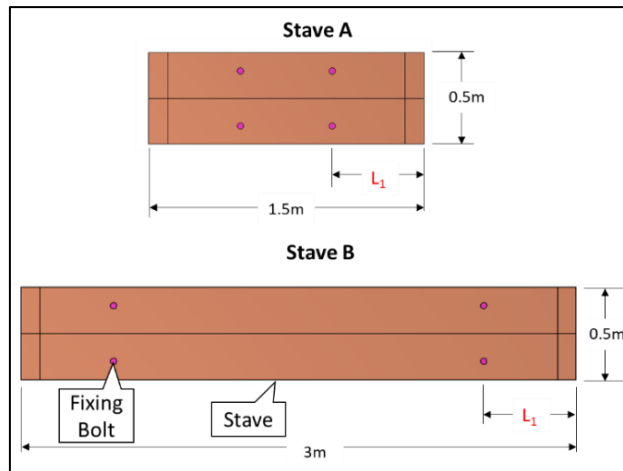


Figure 3. Considered stave geometries

The developed model was used to estimate the stave behavior under thermal cyclic loading scenarios. The stave geometry and mounting supports were compared, and the extent of deformation, stress, and creep strain was analyzed. Bolt forces were analyzed under different heat loading scenarios, which are important for bolt design against fatigue failure.

2.2.1 Boundary Conditions

Mechanical boundary conditions were applied to the stave to simulate the constraints caused by the bolts, pins, gravity, and abrasion forces. The selected stave design includes one locating pin to position the stave onto the blast furnace shell with a tight tolerance fit. Cooling pipes were omitted from the model, assuming a design using expansion joints and flexible collars was employed to minimize stiffness. Applied loads included stave self-gravity and contact pressures caused by the burden. The selected copper staves are also supported by grout, inserted between the blast furnace shell and stave cold face.

The staves are water-cooled, which was modeled using a convection coefficient calculated based on typical plant water temperatures, flow rate, and pipe geometry. The cyclic thermal conditions applied on the stave models were determined using historic thermocouple temperature data from an operating blast furnace plant. The different operating conditions were expressed using their corresponding uniform heat flux values. The minimum and maximum heat flux calculated using thermocouple data are 50 and 400 kW/m², respectively. The maximum heat load of 400 kW/m² is comparable to the maximum heat loads for copper staves reported in literature [2] [3].

An extreme scenario using a heat flux of 1000 kW/m² was checked, representing a case of no refractory and a complete loss of accretion due to high furnace heat load. This was considered as an anomalous case that may occur rarely over the lifetime of a stave. Under such an extreme scenario, nucleate boiling was predicted by the thermomechanical model, a case which was also reported in the field.

2.2.2 Stave Behavior

Copper staves are subjected to variable thermal conditions during operation. Two thermal heat flux cycles were analyzed for each stave; one with a cyclic heat flux to 400 kW/m², and one where the heat flux reaches 1000 kW/m².

2.3 Results

2.3.1 Low Heat Load Cycling

The effect of stave size was evaluated by comparing stave A and B. Figure 4 shows the deformation of the staves when they were subjected to a maximum heat load of 400 kW/m². The staves do not exhibit significant banana effect. This suggests that minimal creep relaxation occurs when exposed to a 400 kW/m² heat load.

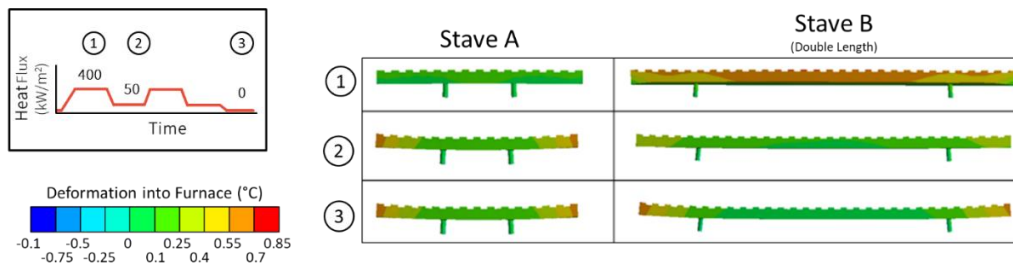


Figure 4. Transient analysis of copper staves under cyclic loading to 400 kW/m² (displacement exaggerated x100)

Figure 5 shows the stress in each stave during this time. For clarity, the ribs of the stave are not shown. The stress distribution in each stave is consistent from cycle-to-cycle.

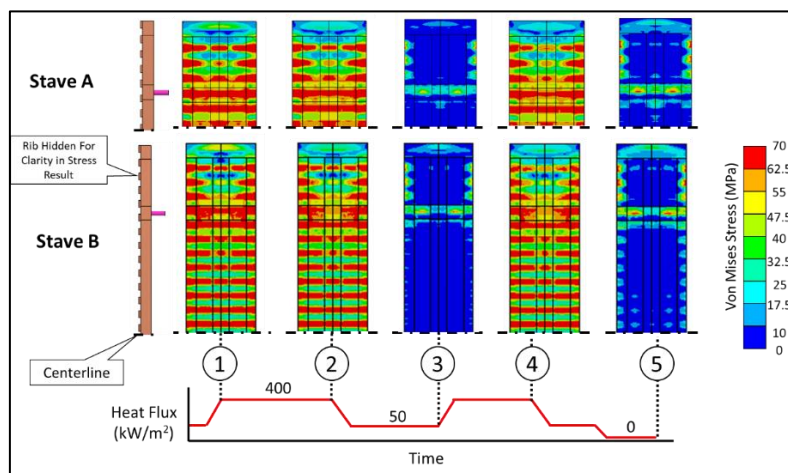


Figure 5. Stress in copper staves heated between 50 and 400 kW/m² during transient analysis. As can be seen in Figure 5, the stress distribution in stave A and stave B are very similar under all conditions. During heating to 400 kW/m², the hot face of the stave experiences high stress. During periods with less extreme heat loading, the stress in the stave is minimal, especially in the center of the stave. This suggests that fatigue cracking of the stave, which is based on the change in stress over a cycle, may be a concern. Further work is required to establish the risk of cracking due to these thermal cycles.

Comparing the stress at time 1, 2, and 4 in Figure 5, the stress distribution in the stave does not change significantly from cycle-to-cycle or over the course of a cycle. This is because creep is not significantly active at the temperatures experienced by the stave. Therefore, stress relaxation in the stave is minimal. This is also consistent with Figure 4, where insignificant banana effect occurs.

2.3.2 High Heat Load Cycling

Figure 6 shows the deformation of both staves when subjected to the extreme thermal condition of 1000 kW/m². Both staves substantially exhibit the banana effect, deforming

more than 5 mm into the blast furnace. This level of deformation was reached after only one cycle to 1000 kW/m². Therefore, even if such heat loading is not captured by the operator, the bending of stave may indicate that a high-heat even occurred in the history of operation.

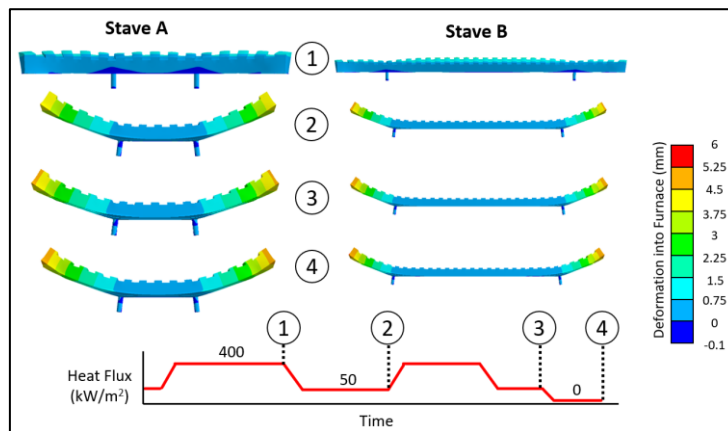


Figure 6. Transient analysis of different-sized copper staves under cyclic loading to 1000 kW/m² (deformation exaggerated x50)

The deformation of the staves increased slightly during the subsequent heating and cooling cycles. This suggests that thermal cycling of the staves can cause progressive damage to the stave. However, further investigation showed that the deformation due to cyclic thermal loading tends asymptotically towards a maximum value. Therefore, the deformation of the stave due to the thermal cycling alone will not cause very large deformations.

One possible explanation for the large banana effect observed in some blast furnaces is the “backfill effect.” Backfilling occurs when burden material deposits/accumulates behind a deformed stave, filling the gap between the grout and restricting stave movement during subsequent thermal cycles [6]. Copper staves experiencing the banana effect may be particularly vulnerable to backfilling because the ends of the staves bend inward, locally disrupting the burden movement and possibly allowing burden materials to flow into the gap created between the stave and the grout.

In Figure 7, the stress distribution in both staves is shown for the case of extreme thermal cycling.

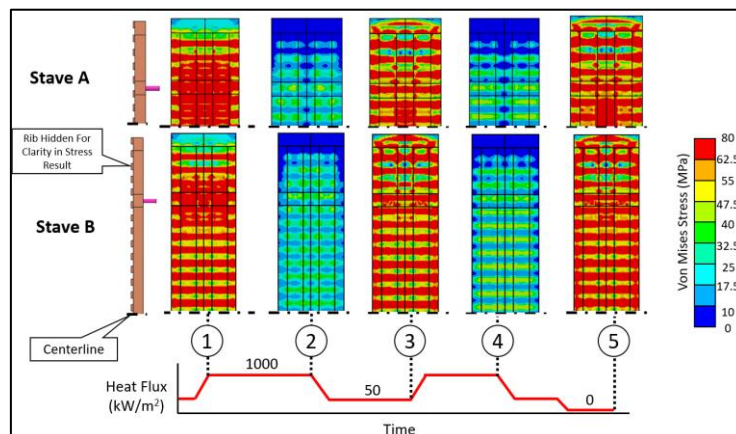


Figure 7. Stress in copper staves heated between 50 and 1000 kW/m² during transient analysis

Stave A and B have very similar stress patterns, suggesting that the overall geometry of the stave is not significant to the stresses developed. Instead, local features such as the stave bolts, ribs, and ends of the stave cause the same stress patterns regardless of stave length.

As can be seen from comparing time 1 and time 2, creep relaxation is occurring in the stave causing a reduction in stress. When the stave cools, residual stress develops as seen at time 3. During the subsequent heating cycle, time 4, the stave returns to a similar stress state as at time 2. This suggests that most of the stress relaxation occurred during the first cycle, and that limited additional stress relaxation and stave deformation will occur. This is consistent with the observed deformations of the stave, which deform asymptotically on subsequent heats.

The deformation observed during one heating event to 1000 kW/m² is less than is observed in some examples. The additional deformation may be due to causes such as the backfill effect, and additional work should be performed to determine possible causes of progressive deformation in staves.

The creep strain of the copper in the Stave A is shown in Figure 8 while the stave is cycled between 50 and 1000 kW/m² conditions.

The areas of the stave with the most significant creep strain are the ribs, which do not have a significant impact on the overall geometric deformation of the stave, and the ends of the stave, which deform substantially because of creep relaxation.

The creep relaxation of a copper stave occurs over a short period of time at high temperatures. This can be seen in Figure 8 by comparing time 1 and time 2. At time 1, the stave has experienced a high heat flux condition for a short period of time. At time 2, the stave has been exposed to the high heat load condition for approximately 5 times longer. Despite the significantly longer period during which creep can occur, only a small amount of additional creep is experienced. Therefore, extended high heat load operation is not required for the banana effect to occur.

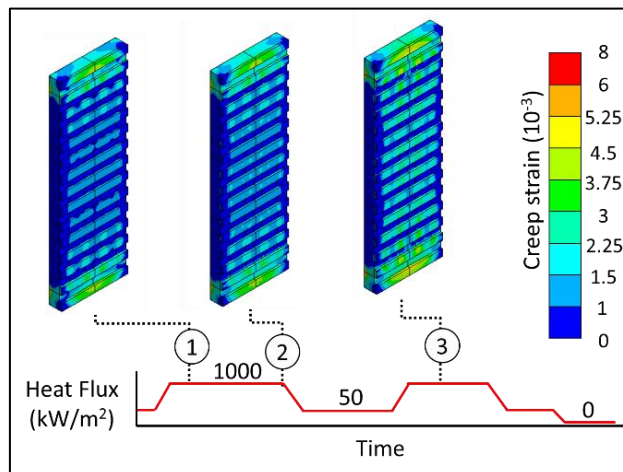


Figure 8. Creep deformation of a stave cycling between 1000 and 50 kW/m²

At time 3, the creep strain in the stave is increased over time 2. This indicates more stress relaxation when the high heat load is resumed, causing the additional deformation of the stave discussed previously. The creep strain in the ribs, combined with cyclic stresses due to thermal cycling, could cause cracking of the hot face of the stave. More work is required to study this possibility in greater detail.

2.4 Discussion

2.4.1 Creep Sensitivity

Creep is an important non-linear behavior which contributes to the stave thermal bending. Creep alters the internal force distribution as creep strains are developed like plasticity. In Figure 9, the region of the stave exposed to creep, above the creep activation temperature of 134°C, is outlined in red [7]. Substantial portions of the stave were shown to be in the creep regime during the high heat flux scenarios.

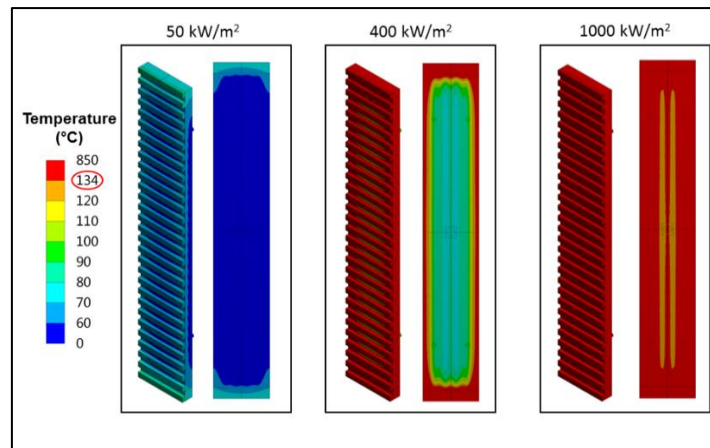


Figure 9. Creep activation for different heat flux scenarios

Since large portions of the stave experienced creep in the high heat flux scenario, the effect of this behavior must be considered. A creep sensitivity analysis was performed using three different creep behaviors: no creep, nominal creep behavior, and creep rate at 10x the nominal rate.

The inclusion of creep in the model has been shown to be extremely important for predicting stave deformation. In the model where creep was excluded, the deformation was underestimated by 70% relative to the case of nominal creep. The results were found to be insensitive to the creep rate. There were only slight differences in creep strain and deformation between the nominal case and the 10x creep rate case. This is because most of the deformation of the stave is due to thermal expansion, a displacement-controlled load. As the stave is held at high temperatures, creep causes stress relaxation, which decreases the magnitude of further creep asymptotically.

2.4.2 Fixing Bolt Fatigue

Cyclic loading scenarios were applied on stave A to examine the fixing bolt loading. Cycles between 50 and either 400 (loading scenario #1) or 1000 kW/m² (scenario #2) were considered. The bolt force generated in each case is shown in Figure 10. A third scenario (#3), in which the stave is subjected to a single 1000 – 50 kW/m² cycle and then cycled repeatedly at 400 – 50 kW/m², is also considered.

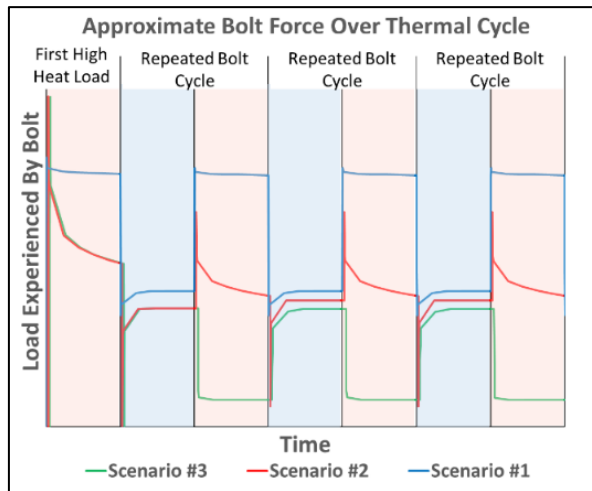


Figure 10. Force applied to fixing bolt during different loading scenarios

As seen in Figure 10, the stress range experienced by the first cycle is higher than for subsequent cycles which all have an approximately equal stress range. The impact of the large first cycle is not significant for bolt fatigue life, so it is not considered for this analysis. The fatigue life of the bolts in each position is given in Table 1.

Table 1. Fatigue life of bolts under different cyclic loading conditions

Scenario	A	B
	Small Stave (cycles to failure)	Large Stave (cycles to failure)
#1 (50-400 kW/m ² Cycle)	5,300	4,000
#2 (50-1000 kW/m ² Cycle)	3,000	2,400
#3 (50-1000 cycle, followed by repeated 50-400 cycle)	20,000	15,000

As can be seen in Table 1, the fatigue life of the bolts is shorter for the larger B staves in all cases. This is due to higher bolt forces in the larger stave. The B stave had only a slightly increased bolt stress - less than 15% in each case - versus the A stave, despite being double the size. Therefore, while the size of the stave has an effect of the bolt force experienced, the size of a stave will probably not be limited by concerns about the bolt force on a stave.

Table 1 also shows that the fatigue of bolts could be an issue in a long-operating blast furnace, depending on the operational stability of the furnace. For instance, the bolts of the B stave have an expected life of ~11 years if they experience a thermal cycle of 50 – 400 kW/m² every day. In a blast furnace with this level of thermal cycling, bolt failure could become a concern during the campaign life of the furnace. In a stave with more stable operating conditions where significant thermal cycles occur infrequently, bolt fatigue may not be an issue even at the end of a 20-year campaign.

As can be seen in Figure 10, the bolt force pattern in each scenario is very different. In Scenario #1, the bolts cycle between a constant high load force (during hot times) and a constant low load (during cold times). In contrast, in Scenario #2 the bolt has a peak maximum or minimum bolt force load during the transition between hot and cold during each cycle, and a moderate bolt load during times of steady hot or cold operation. The

bolts experience a lower maximum load in Scenario #2 compared to Scenario #1 (except for the first cycle), due to stress relaxation reducing the load on the bolts. However, Scenario #2 is most critical for fatigue because the bolts experience the greatest stress range in this scenario.

In Scenario #3, the initial cycle between 50 and 1000 kW/m² causes significant changes to the bolt loading pattern versus a stave that did not experience this initial cycle (i.e. Scenario #1). This first extreme cycle results in an increase in the expected life of the stave bolt versus if the extreme cycle had not occurred.

These findings demonstrate that the fatigue load of a bolt is highly dependent on the historical thermal loads. More work is required to determine consistent patterns in bolt loading based on stave history; for instance, extreme thermal loads in a stave may not always tend to reduce the bolt load on subsequent less-extreme cycles. These findings also demonstrate that a complete time history of a stave is important for diagnosis of issues with stave bolts.

2.4.3 Bolt Failure

If the bolts fail due to fatigue or other mechanical issues, they will no longer restrict the stave deformation. All staves were analyzed to determine the deformation if a pair of fixing bolts - either the top or bottom pair - were to fail.

The staves analyzed previously, Stave A and Stave B, had fixing bolts located a constant distance from the end of each stave to demonstrate that the banana effect occurs on material outside of the fixing bolts. A new stave, Stave C, with the same length as Stave B but a narrower spacing between the bolts (the same as Stave A), is also considered for this case.

The staves experienced a cyclic load between 50 and 1000 kW/m², then the mechanical boundary conditions of the model were adjusted to represent the condition of a stave after bolt failure. The deformation for each stave is shown in Figure 11 before and after the failure occurred.

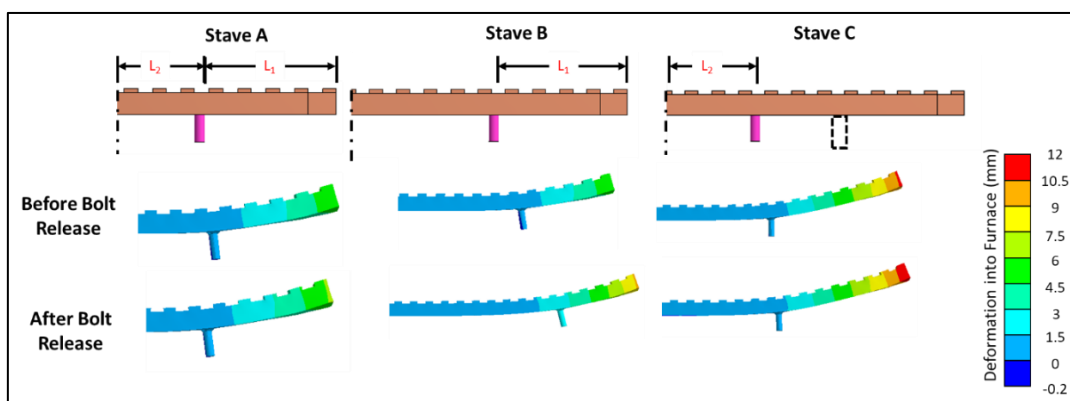


Figure 11. Effect of bolt failure on deformation

Before the bolt failure occurred, Stave C had a larger deformation than Stave A or B since it had a larger amount of material beyond the bolts in which banana effect deformation would occur.

When bolt failure occurred, Stave B experienced an increase in maximum deformation of approximately 30%. The end of the stave bends further into the furnace. Stave A and Stave C both experienced substantially less additional deformation (around 1 mm or 8%). This suggests that the additional bending due to a bolt failure is due to the additional bending of the previously undeformed middle section of the stave.

The additional deformation that may occur after a bolt fails can have ramifications for the stave life. For instance, cooling pipes on the stave may exceed the limit of their expansion joints due to stave bending. This finding also has consequences for the forensic investigation of a deformed stave; when the stave is removed from the furnace, its deformation will increase. Therefore, any examination of the stave bending deformation and corresponding stave failure must consider that the observed deformation is greater than that which occurred during operation.

3 CONCLUSION

A methodology for simulating the behavior of a blast furnace copper stave was developed, accounting for copper's temperature-dependent material properties, including plasticity and creep. The creep effect, typically not considered in the literature, is critical for determining the full extent of deformation especially in high heat loads and large stave cases. This methodology can be used to explain and predict various stave failure mechanisms such as bolt failure and the banana effect, and may also be able to provide insight into the cracking of stave hot faces due to thermal cycling.

The banana effect in copper staves was investigated in depth. The bending deformation of the stave depends on the maximum heat load that the stave experiences and the stave fixing bolt location, with bolts located closer to the edges of the stave producing less deformation. It was found that a single high-temperature event could cause significant deformation to the copper stave. The deformation was expected to increase if the backfill effect of the burden materials was considered.

Cyclic thermal loading of the stave results in high cyclic force loads in the fixing bolts, which can cause fatigue damage and needs to be considered in the initial design. The developed stave model can be used to evaluate the effect of bolt failure on the increased deformation of the stave. The condition of the grout has an important influence on the initial deformation behavior of the stave, with a stiff grout being essential for the banana effect to occur at its early stages.

The observed deformation of the stave can be linked to several failure modes. The cyclic loading of the stave can cause the fixing bolts to fail in fatigue, leading to even greater deformation. The deformation at the ends of the stave can cause high cyclic loading and cracking of the water pipe if not properly considered in design, leading to water leaks.

The historic conditions that a stave is exposed to are critical in determining the current state of a stave. A single high-heat event can cause significant, irreversible deformation to the stave, radically changing the stress-state of the stave material and affect the fatigue damage caused by subsequent cycling of the stave fixing bolts.

REFERENCES

- 1 G. Cegna, O. Lingiardi and R. Musante, "Copper Staves Wear — Ternium Siderar BF2 Experience," in 2014 AISTech Conference Proceedings, Indianapolis, 2014.

- 2 R. Janjua, Y. De Langhe, M. Esmer, R. Musante, G. Catalá and B. Jansson, "Life extension of Copper Staves in Blast Furnaces," in METEC & 2nd ESTAD, Düsseldorf, 2015.
- 3 S. Lin and C. Fu jun, "The Research on Creep Deformation and Thermal Stress of Cast Copper Staves," Applied Mechanics and Materials, Vols. 325-326, pp. 336-339, 2013.
- 4 Q. Liu and S. Cheng, "Heat transfer and thermal deformation analyses of a copper stave used in the belly and lower shaft area of a blast furnace," International Journal of Thermal Sciences, no. 100, pp. 202-212, 2016.
- 5 KME, "Copper Staves for Blast Furnaces," 2016. [Online]. Available: http://www.kme.com/fileadmin/DOWNLOADCENTER/SPECIAL%20DIVISION/1%20Melting%20%26%20Casting/3%20Products/7%20Cooling%20Elements/Copper_Staves_For_Blast_Furnaces_2016.pdf. [Accessed 8 December 2017].
- 6 M. Esmer, H. A. Özyigit, R. Janjua, G. Catala, R. Musante and B. Jansson, "A New Practical Engineering Approach to Improving the Service Reliability of Copper Staves in Blast Furnaces," in 3rd ESTAD, Vienna, Austria, 2017.
- 7 J.-l. Zhang, Y.-x. Chen, Z.-y. Fan, Z.-w. Hu, T.-j. Yang and T. Ariyama, "Influence of Profile of Blast Furnace on Motion and Stress of Burden by 3D-DEM," Journal of Iron and Steel Research, International, vol. 18, no. 11, pp. 1-6, 2011.
- 8 W. H. Bower, "Creep of the Copper Canister: A Critical Review of the Literature," SKI, Surry, UK, 2003.